Video Article

Imaging Local Ca^{2+} Signals in Cultured Mammalian Cells

Jeffrey T. Lock[1], Kyle L. Ellefsen[1], Bret Settle[1], Ian Parker[1,2], Ian F. Smith[1]

[1]Neurobiology and Behavior, University of California, Irvine

[2]Physiology and Biophysics, University of California, Irvine

Correspondence to: Ian F. Smith at ismith@uci.edu

Abstract

Cytosolic Ca^{2+} ions regulate numerous aspects of cellular activity in almost all cell types, controlling processes as wide-ranging as gene transcription, electrical excitability and cell proliferation. The diversity and specificity of Ca^{2+} signaling derives from mechanisms by which Ca^{2+} signals are generated to act over different time and spatial scales, ranging from cell-wide oscillations and waves occurring over the periods of minutes to local transient Ca^{2+} microdomains (Ca^{2+} puffs) lasting milliseconds. Recent advances in electron multiplied CCD (EMCCD) cameras now allow for imaging of local Ca^{2+} signals with a 128 x 128 pixel spatial resolution at rates of >500 frames sec^{-1} (fps). This approach is highly parallel and enables the simultaneous monitoring of hundreds of channels or puff sites in a single experiment. However, the vast amounts of data generated (*ca.* 1 Gb per min) render visual identification and analysis of local Ca^{2+} events impracticable. Here we describe and demonstrate the procedures for the acquisition, detection, and analysis of local IP$_3$-mediated Ca^{2+} signals in intact mammalian cells loaded with Ca^{2+} indicators using both wide-field epi-fluorescence (WF) and total internal reflection fluorescence (TIRF) microscopy. Furthermore, we describe an algorithm developed within the open-source software environment Python that automates the identification and analysis of these local Ca^{2+} signals. The algorithm localizes sites of Ca^{2+} release with sub-pixel resolution; allows user review of data; and outputs time sequences of fluorescence ratio signals together with amplitude and kinetic data in an Excel-compatible table.

Video Link

The video component of this article can be found at http://www.jove.com/video/52516/

Introduction

Calcium ions (Ca^{2+}) ubiquitously regulate a diverse range of biological processes, including gene expression, secretion and long-lasting changes in synaptic plasticity[1]. One way through which Ca^{2+} can act in such a diverse manner is through the different spatial and temporal patterns of Ca^{2+} signals a cell can generate. For example global elevations in cytosolic [Ca^{2+}] trigger contraction in smooth muscle tissue[2] whereas smaller, localized transient elevations (local Ca^{2+} microdomains) stimulate gene expression essential for learning and memory[3].

Free cytosolic [Ca^{2+}] is maintained at ~100 nM at rest, but can rapidly rise to several micro-molar following the influx of Ca^{2+} into the cytosol through Ca^{2+}-permeable ion channels located in the plasma membrane and by the liberation of Ca^{2+} from intracellular stores. Our lab focuses on the inositol 1,4,5-trisphosphate receptor (IP$_3$R), which forms a Ca^{2+} release channel located in the endoplasmic reticulum (ER) membrane. Upon binding of both IP$_3$ and Ca^{2+} to the cytosolic activating sites of the receptor, the IP$_3$R channel opens to liberate Ca^{2+} sequestered within the ER lumen. The release of Ca^{2+} may remain spatially restricted to a small cluster of IP$_3$Rs to generate a local cytosolic microdomain of Ca^{2+} (Ca^{2+} puff[4]) or, depending on the proximity of neighboring clusters of IP$_3$Rs, may propagate throughout a cell by recruiting multiple puff sites through a process of Ca^{2+}-induced Ca^{2+}-release (CICR)[5,6].

The introduction of fluorescent small molecule Ca^{2+} indicator dyes developed by Roger Tsien[7], coupled with advanced microscopy imaging techniques, has greatly facilitated our understanding of Ca^{2+} signaling. Recent advances in cameras used for microscopy now allow for imaging transient local Ca^{2+} events such as puffs with unprecedented spatial and temporal resolution. Currently available EMCCD cameras enable imaging with 128 x 128 pixels at >500 frames sec^{-1} (fps) and the new generation of complementary metal-oxide semiconductor (CMOS) cameras provide higher pixel resolution, and even faster speed at the expense of slightly higher noise levels. In conjunction with total internal reflection (TIRF) microscopy it is now possible to image single Ca^{2+} channel events[8,9]. This approach allows for the imaging of hundreds of channels/ events simultaneously, while generating large data sets (*ca.* 1Gb per min) that render manual processing, visual identification and analysis impracticable and place an onus on the development of automated algorithms.

Here, we present procedures and protocols for imaging local Ca^{2+} signals in intact mammalian cells using fluorescent Ca^{2+} indicators. We further demonstrate an algorithm developed in the open-source environment Python that automates identification and analysis of local Ca^{2+} events imaged by both TIRF and conventional wide field epi-fluorescence (WF) microscopy. Although we describe these approaches in the context of

IP$_3$-generated Ca^{2+} signals, they are readily amenable to study local changes in cytosolic [Ca^{2+}] emanating from a variety of Ca^{2+}-permeable ion channels located in either the surface membrane or intracellular organelles[8-10].

Protocol

We present detailed procedures for imaging local Ca^{2+} events in human neuroblastoma SH-SY5Y cells. These procedures can be adapted to image intracellular Ca^{2+} signals in many cell types[8-10].

1. Preparation of Cells

1. Culture the cells to be imaged according to instructions listed on their supplier's website.
2. A few days prior to imaging, harvest cells grown in a tissue culture flask using 1 ml of 0.25% Trypsin/EDTA (2-3 min). Following detachment, add an equal volume of culture media to inactivate the trypsin.
3. Perform a cell count using a hemocytometer and seed cells into glass-bottom imaging dishes at a density of 3-7 x 10^4 cells per dish. Select cells for imaging experiments when they reach 60% confluence (2-3 days).

2. Preparation of Solutions and Reagents

1. Prepare a Ca^{2+}-containing HEPES buffered salt solution (Ca^{2+}-HBSS) composed of (mM): 135 NaCl, 5.4 KCl, 2 CaCl$_2$, 1 MgCl$_2$, 10 HEPES, and 10 glucose; pH=7.4 at room temperature (RT) with NaOH. Prepare Ca^{2+}-HBSS without the addition of glucose and store at 4 °C; add glucose to the solution immediately prior to use.
2. Solubilize membrane-permeant forms of the fluorescent Ca^{2+} indicator Cal-520 (1 mM), ci-IP$_3$ (200 µM), and EGTA (100 mM) in dimethyl sulfoxide (DMSO) containing 20% pluronic F-127. Aliquot these reagents into Eppendorf tubes and store, shielded from moisture and light, at -20 °C.

3. Loading Cells with Membrane-permeant Cal-520, ci-IP$_3$ and EGTA

1. Prepare the "loading buffer" by diluting stock solutions of membrane-permeant Cal-520 and ci-IP$_3$ to a final concentration of 5 µM and 1 µM, respectively, in Ca^{2+}-HBSS.
2. Aspirate culture media and rinse cells by replacing media with Ca^{2+}-HBSS three times.
3. Remove Ca^{2+}-HBSS and incubate cells in loading buffer for 60 min at RT in the dark.
4. Remove loading buffer and rinse cells by replacing media with Ca^{2+}-HBSS three times.
    1. If desired, at this step, load cells with EGTA/AM by diluting the stock solution to a final concentration of 5 µM in Ca^{2+}-HBSS and then incubate cells for 30-60 min at RT in the dark. Following this incubation, rinse cells three times with Ca^{2+}-HBSS before proceeding to step 3.5.
5. Incubate cells in Ca^{2+}-HBSS for 30 min to allow for de-esterification of loaded reagents.
6. Immediately prior to imaging, replace Ca^{2+}-HBSS with "fresh" Ca^{2+}-HBSS in order to remove any dye that might have leaked into the bath during the final incubation.

4. Ca^{2+} Image Acquisition

1. Place a small drop of immersion oil onto the 100X APO TIRF objective (NA 1.49).
2. Mount the imaging dish on the stage of the inverted microscope and bring the cells into focus using transmitted light. It is important to secure the imaging dish to prevent movement during recording.
3. Illuminate cells with a 488 nm laser in order to excite Cal-520 and collect emitted fluorescence (λ >510 nm) using a high-speed EMCCD camera.
   NOTE: The software package that operates the microscope allows the user to translate a focusing lens allowing the laser beam to be introduced either at the extreme edge of the objective back aperture (for TIRF excitation) or more centrally (for "WF" excitation).
4. Using the EMCCD software, reduce the imaging field from the full 512 x 512 pixels in order to collect data at the necessary temporal resolution to capture local Ca^{2+} events.
   NOTE: For example, center quad acquisition of 256 x 256 pixels speeds up the acquisition rate to 66 fps. It is also possible to further increase the frame rate of the EMCCD camera to 500 fps using an Isolated Crop Mode function.
5. Configure the software to automatically record a few seconds of baseline activity, deliver a UV flash to the cells and continue recording for another 10-30 sec.
   NOTE: A UV flash is delivered using a Xenon arc light source introduced through a UV reflecting dichroic mirror in the rear port of the microscope. The duration and intensity of the UV flash is adjusted empirically to evoke a desired frequency of local Ca^{2+} events.
6. Save files as image stacks for off-line analysis.

5. Automated Ca^{2+} Image Analysis

NOTE: It is possible to view, process and analyze captured data using many commercial software packages. However, we have developed an algorithm to rapidly automate identification and analysis of local Ca^{2+} signals. A detailed description of the spatial and temporal filters used in this algorithm, generation of the ΔF/F$_0$ and identification/analysis routines can be found in[11]. This algorithm has been developed to run on the open-

source software platform Python, and can be obtained, together with sample experimental data and detailed user instructions, by e-mailing the corresponding author (ismith@uci.edu).

1. Convert files to be imported into the custom-written algorithm to the multi-plane .tiff file format.
2. Locate the folder containing the analysis algorithm and double click the run.exe.
3. Select the .tiff file to be analyzed.
4. Choose analysis parameters in the open dialog box. See **Figure 2A** for default parameters for the sample data.
5. Determine the black level to be offset from the image stack by either moving the cursor to a part of the field of view that does not contain a cell (see **Figure 2B**) or by manually entering a black level using the 'Set Black Level' prompt.
6. Observe four windows on the screen following analysis by the software (**Figure 2C-F**). C is a monochrome image of resting fluorescence from cells being analyzed. White squares superimposed on this image are event locations, determined as the centroid positions of two-dimensional Gaussian functions fitted to events.
7. Click on each event location or press the cursor keys to cycle between events. Upon doing so the background-subtracted, Gaussian smoothed fluorescence ratio changes ($\Delta F/F_0$) at each of these sites update in window D.
   NOTE: Red highlighted events are determined to originate from that particular site and not from 'bleed-through' from activity localized to adjacent sites. The lower blue trace indicates where the fluorescence signal at the selected site exceeded the detection threshold, whereas the black line identifies events originating from that particular site (corresponding to the red highlighted events).
8. Click on a red highlighted event to update window E that displays the temporal evolution of the event, and window F which displays the spatial profile of the event averaged over its time course, together with the spatial profile of the fitted Gaussian function.
9. Manually review the events that have been identified so that artifacts can be rejected from analysis. Delete such events by right clicking the red highlighted events.
   NOTE: In our hands, Ca^{2+} flux through single IP_3R channels evokes signals with $\Delta F/F_0$ about 0.11, so any detected 'events' appreciably smaller than this are likely to be false positives.
10. Export data by selecting 'Save to Excel' or export data on a per cell basis by drawing around the cell of interest and selecting 'Save Cell'.
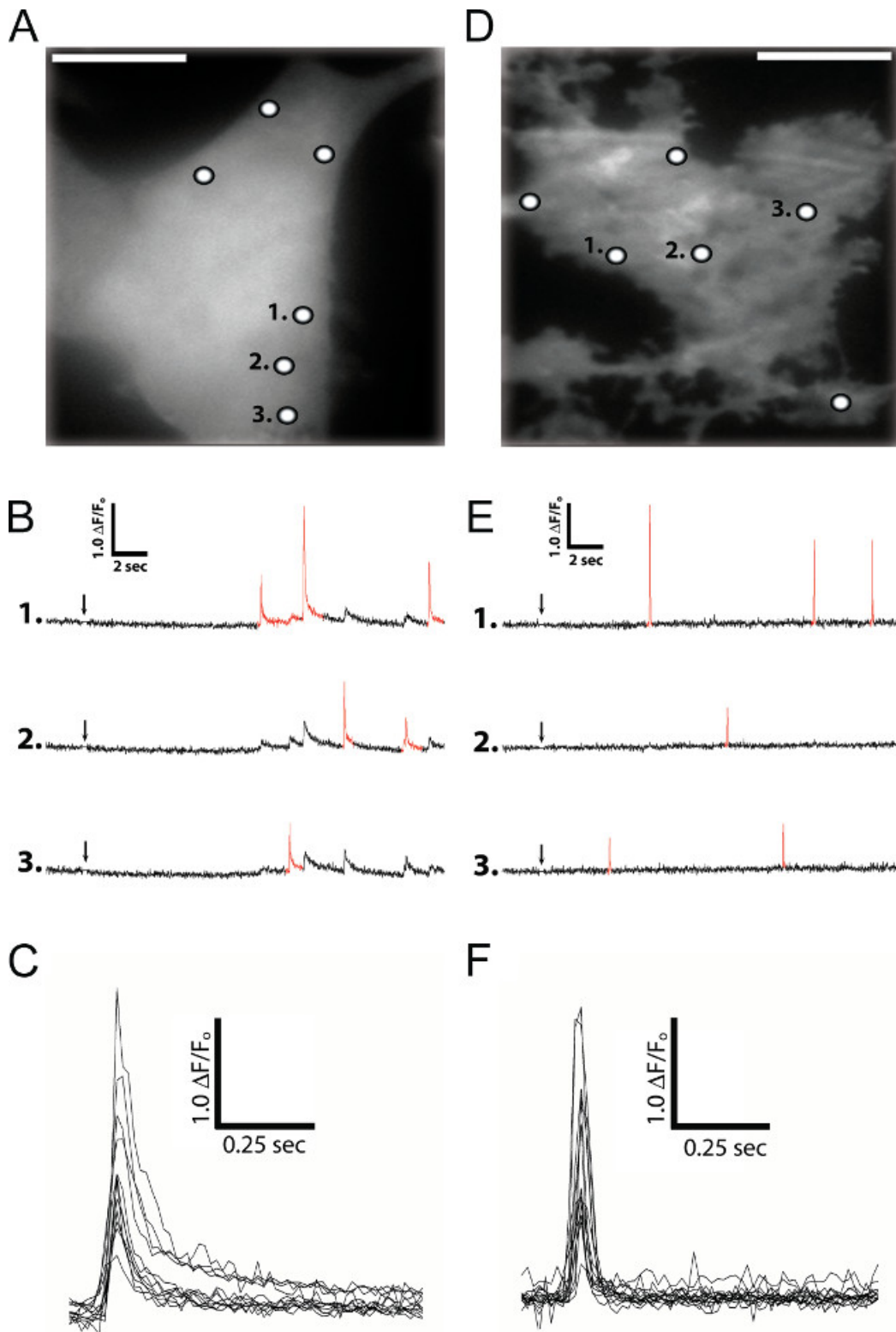   NOTE: Data are saved to the same folder as the original image stack.

Representative Results

Figure 1A shows a WF image of resting Cal-520 fluorescence in human neuroblastoma SH-SY5Y cells also loaded with ci-IP_3. Exposure of these cells to a 100 msec UV flash to photo-release i-IP_3 elicited transient Ca^{2+} puffs at discrete sites (noted by the white circles in **Figure 1A**). Fluorescence traces measured at these sites showed a rapid rising phase owing to transient openings of IP_3Rs, followed by a much slower falling phase (**Figure 1B** and **1C**) as Ca^{2+} slowly diffused away from the release site. Red highlighted events in **Figure 1B** are Ca^{2+} signals that were determined by the algorithm to have originated from the selected site. Non-highlighted events represent contaminating Ca^{2+} signals diffusing from closely adjacent sites.
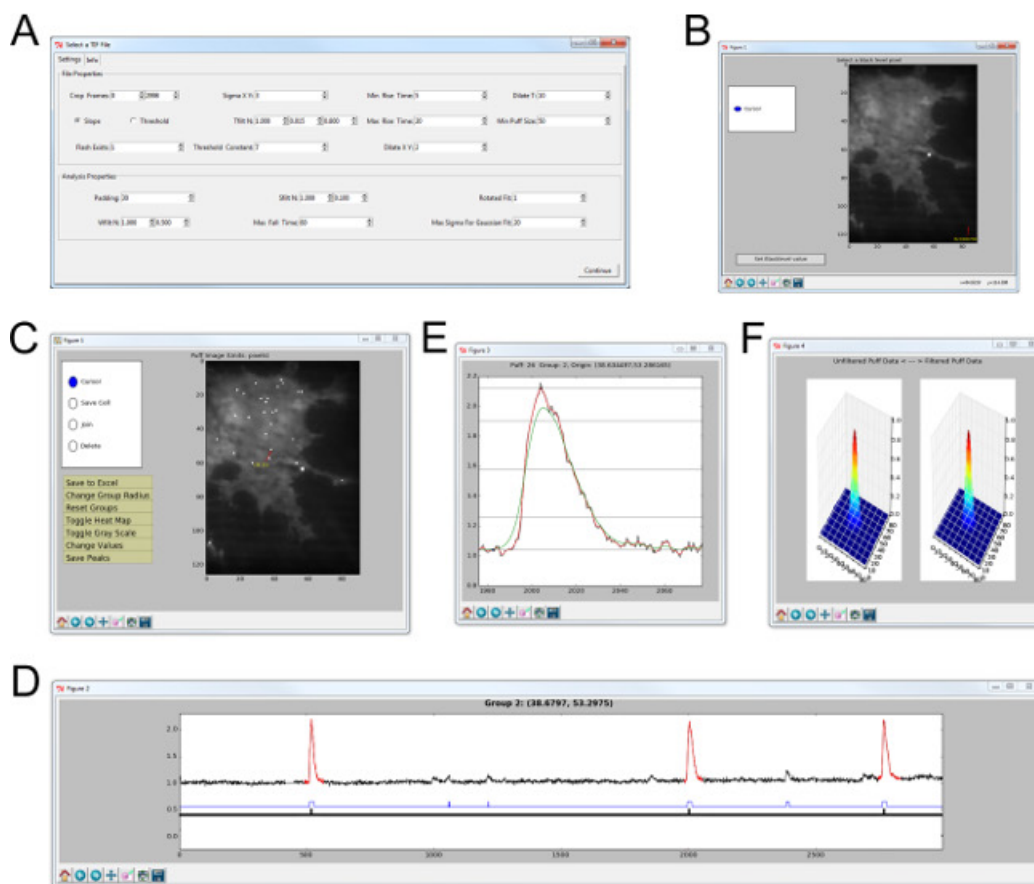
To achieve higher-resolution imaging of local Ca^{2+} signals, cells may be further loaded with the slow Ca^{2+} buffer EGTA. This chelates Ca^{2+} ions diffusing between puff sites and thus prevents the generation of global Ca^{2+} waves that would obfuscate the study of local Ca^{2+} puffs generated by individual clusters of IP_3Rs. Furthermore, EGTA accelerates the collapse of the local Ca^{2+} microdomain but, owing to its slow binding kinetics, minimally perturbs local free Ca^{2+} and its binding to the fast Ca^{2+} indicator within a cluster. The net effect of EGTA is to 'sharpen' fluorescence records of puffs in space and time, without appreciably diminishing their amplitude. A further improvement in resolution arises by using TIRF to limit excitation of the Cal-520 fluorophores to the narrow (<100 nm) evanescent wave created by TIRF. The sum of both of these approaches is a technique that effectively monitors instantaneous Ca^{2+} release flux (Ca^{2+} current) rather than a leaky integral of Ca^{2+} after it is released through the IP_3Rs and slowly diffuses away from the release site and is ultimately sequestered [9]. **Figure 1D** shows the TIRF 'footprint' of an SH-SY5Y cell when Cal-520 fluorophores were only excited within a narrow distance into the cell from the coverglass/aqueous solution interface. Rapid binding of Ca^{2+} to the fast indicator Cal-520 dye within the attoliter cytosolic volumes created by TIRF illumination, in conjunction with EGTA to 'mop' up diffusive Ca^{2+}, yields fluorescence signals that are sharpened in both time and space (**Figure 1E** and **1F**).

The analysis of image stacks captured in this manner is greatly facilitated through a custom written algorithm developed in our lab running on the open-source software platform Python[11]. **Figure 2A** shows the opening dialog window in which the user enters parameters to be used for identification and subsequent analysis of image stacks. Following this, the user is prompted to select a black level to be subtracted from the entire image stack after which the identification and analysis algorithm runs. **Figure 2C-F** show, respectively, the subcellular sites of local Ca^{2+} release; activity at selected sites; individual events on an expanded timescale; and spatial profiles of representative events (see **Figure 2** legend for details). Upon user review of identified sites, analyzed data for all events (see **Table 1**) can be exported by selecting the 'Save to Excel' function.
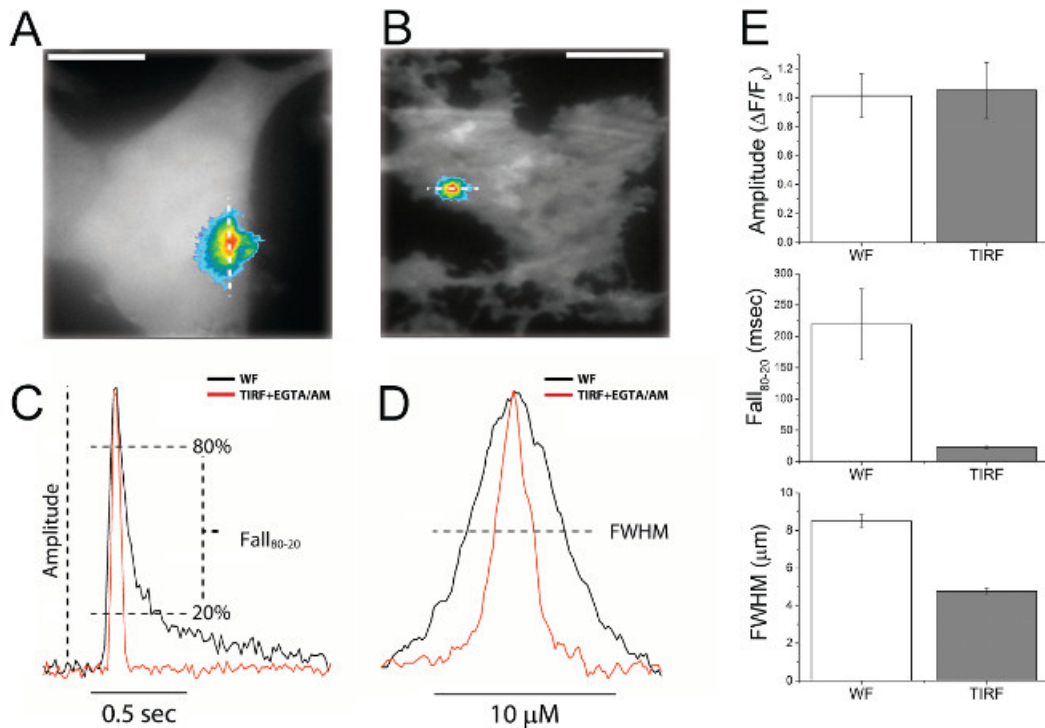
Figure 3 presents data illustrating both the improvement in resolution achieved by TIRF imaging in EGTA-loaded cells as compared to WF imaging in unloaded cells, and the power of the algorithm in identifying and analyzing local Ca^{2+} signals. **Figure 3A** shows a representative local event imaged by WF in a cell loaded only with Cal-520 and ci-IP_3. For comparison, **Figure 3B** shows an analogous event but now imaged by TIRF microscopy in a cell further loaded with EGTA. Superimposed traces in **Figure 3C** and **3D**, illustrate corresponding temporal (C) and spatial (D) profiles of events recorded by WF fluorescence without EGTA (black) and by TIRF microscopy with EGTA loading (red). **Figure 3E** plots mean measurements of puff amplitudes, decay times, and spatial width under these two conditions, determined using the algorithm to analyze approximately 44 (WF) and 88 (TIRF) events.

Figure 1: IP$_3$-evoked local Ca^{2+} signals in SH-SY5Y cells loaded with Cal-520 and ci-IP$_3$ imaged by wide-field (A through C) and TIRF (D through F) microscopy. (A) Monochrome image of resting Cal-520 fluorescence on which puff site locations are denoted by white circles; scale bar = 10 µm. **(B)** Traces illustrate puffs evoked at three different sites, numbered as in (A). Red highlighted events are puffs identified to have originated from that particular site. Arrow indicates time of UV flash. **(C)** Superimposed traces of representative Ca^{2+} puffs like those in (B), aligned and shown on an expanded scale. **(D)** Monochrome TIRF 'footprint' image of resting Cal-520 fluorescence in SH-SY5Y cells loaded with ci-IP$_3$ and EGTA. White circles denote puff site origins. **(E)** Traces illustrate puffs evoked at three different sites numbered as in (D). **(F)** Superimposed traces of representative Ca^{2+} puffs like those in (E), aligned and shown on an expanded scale.

Figure 2: User interface of custom code designed to automatically identify and analyze local Ca^{2+} signals in SH-SY5Y cells imaged by TIRF microscopy. (A) Opening dialog box where identification and analysis parameters are entered. **(B)** The user selects a region of the image that contains no cells to define the black level that is subtracted from the all frames in the image stack. **(C-F)** Screenshots of the final/ identification analysis windows. **(C)** Image of resting Cal-520 fluorescence on which are superimposed locations where Ca^{2+} transients were identified (white squares). The user can cycle between sites by moving the mouse over the image or pressing the cursor keys. **(D)** Window showing fluorescence ratio ($\Delta F/F_0$) trace at the selected event. Red-highlighted events are identified as having arisen at the site selected. The lower blue bar indicates events that exceed the threshold for detection at that site; events not highlighted red have been localized to an adjacent site. Clicking on the blue bar takes the user to that event site. Clicking on a red event with the mouse opens up two further windows showing the temporal evolution of the event on an expanded timescale **(E)** and spatial profiles **(F)** of the event averaged over its time course (left) together with the spatial profile of the fitted Gaussian (right). Please click here to view a larger version of this figure.

Figure 3: Improvement in temporal and spatial fidelity of puff imaging achieved by use of TIRF microscopy in conjunction with intracellular loading of EGTA. (A) snapshot image of a puff captured at time of peak amplitude, superimposed on a background image of resting fluorescence to show the cell outline. The image was obtained by WF microscopy of a cell not loaded with EGTA. The puff image is pseudocolored, with higher Ca^{2+} levels denoted by increasingly 'warm' colors. (B) Corresponding image of a puff imaged by TIRF microscopy in a cell loaded with EGTA. (C) Traces, WF (black) or TIRF + EGTA (red), show the corresponding change in Cal-520 fluorescence over time for the Ca^{2+} puffs shown in (A) and (B) above. Traces are normalized to the same peak amplitude and aligned to their peak time to facilitate comparison of their kinetics. Annotations illustrate measurements of Ca^{2+} event parameters (amplitude and fall time) quantified in (E). (D) Traces, WF (black) or TIRF+EGTA (red), show the fluorescence intensity of a line scan through the Ca^{2+} puffs shown in (A) and (B). Line scans are normalized to their peak amplitudes, and centered. The annotation shows measurement of full width at half maximal amplitude (FWHM), as quantified in (E). (E) Bar graphs showing mean peak amplitudes (top), fall times from 80% to 20% of peak amplitude (middle), and spatial width (FWHM) of puffs imaged by WF microscopy in cells without EGTA (open bars) and by TIRF microscopy in EGTA-loaded cells (grey bars). Data are presented as mean ± SEM with an n of at least 37 puffs for WF and 79 for TIRF. Please click here to view a larger version of this figure.

A.	Group #	Event site identity number
B.	GroupX:	Mean sub-pixel x location of all events at a particular site
C.	GroupY:	Mean sub-pixel y location of all events at a particular site
D.	No. Events:	No. of events occurring at a site over the course of the experiment.
E.	Max Amp:	Maximum amplitude of an event at that particular site ($\Delta F/F_0$)
F.	X:	Sub-pixel x localization of event
G.	Y:	Sub-pixel y localization of event
H.	T_peak:	Time at which the event reaches peak amplitude (in frame number)
I.	Amplitude:	Amplitude of all events originating from each site ($\Delta F/F_0$)
J.	Sigmax:	X SD of Gaussian profile fitted to time course of event (in pixels)
K.	Sigmay:	Y SD of Gaussian profile fitted to time course of event (in pixels)
L.	Angle:	Angle of the long axis of the resulting elliptical function of Gaussian fitted to time course of event
M.	R20:	Time to rise to 20% of max amplitude (in frames)
N.	R50:	Time to rise to 50% of max amplitude (in frames)
O.	R80:	Time to rise to 80% of max amplitude (in frames)
P.	R100:	Time to rise to 100% of max amplitude (in frames)
Q.	F80:	Time to Fall to 80% of max amplitude (in frames)
R.	F50:	Time to Fall to 50% of max amplitude (in frames)
S.	F20:	Time to Fall to 20% of max amplitude (in frames)
T.	F0:	Time to return to pre-event baseline (in frames)

Table 1: Output data from algorithm.

Discussion

We describe here protocols for imaging local Ca^{2+} events in cultured mammalian cells using fluorescent Ca^{2+} indicators. Furthermore, we describe an algorithm with an intuitive user interface that automates identification and analysis of acquired data. The procedure described here utilize the fluorescent Ca^{2+} indicator Cal-520, but many other Ca^{2+} sensitive dyes such as Fluo-3, Fluo-4, Fluo-8 and Oregon Green BAPTA-1 perform sufficiently well to image Ca^{2+} microdomains. Care does need to be taken to ensure that the high affinity versions (K_d of ~200-400 nM) of these indicators are used to image local Ca^{2+} microdomains, and the optimal loading conditions of these indicators need to be determined empirically for each cell type under investigation. By their nature Ca^{2+} indicators bind Ca^{2+} and thus act as Ca^{2+} buffers; higher loading concentrations of indicators have the potential to interfere with Ca^{2+} signals being recorded and/or may be sequestered into intracellular organelles, although the loading conditions described here are a good starting point. Overall, imaging the activity of local Ca^{2+} events is minimally invasive, maintaining the native architecture of a cell and cytosolic factors that may regulate the channels that underlie Ca^{2+} microdomains.

The protocol we describe here for high-resolution imaging of local Ca^{2+} signals using TIRF microscopy has the obvious limitation in that it restricts measurements to events that arise from Ca^{2+} channels lying within the evanescent field. However, it is not restricted only to channels in the plasma membrane, and we demonstrate its applicability to channels such as the IP_3R in intracellular organelles that have been found to be preferentially located close to the plasma membrane[12] but would otherwise be inaccessible to electrophysiological recording of their activity in the native cellular environment. Confocal imaging would enable imaging of signals generated deeper into the cell, but has disadvantages as compared to TIRF imaging in that the thickness of the optical section is wider (~800 nm vs 100-200 nm) and is limited in temporal resolution by

the need to scan the confocal spot(s). Because imaging is done in an epi-fluorescence mode using an inverted microscope, optical recordings of local and single-channel Ca^{2+} signals could readily be combined with simultaneous electrophysiological patch-clamp recording.

By expressing fluorescence Ca^{2+} signals as a ratio of resting fluorescence ($\Delta F/F_0$) it is possible to obtain a good *relative* measure of signal amplitudes. However, we caution that calibration of local, transient fluorescence changes in terms of absolute Ca^{2+} concentrations is not appropriate. The gradients of free $[Ca^{2+}]$ and Ca^{2+}-bound indicator around a Ca^{2+} release channel or cluster of channels is narrower than can be resolved by optical microscopy and will thus be blurred by the point spread function of the microscope. Moreover, local $[Ca^{2+}]$ in the close vicinity of the channel pore will change on a microsecond timescale as the channel opens and closes. Thus, the fluorescence signals provide only a blurred (in space and time) representation of the true Ca^{2+} nanodomain underlying local Ca^{2+} signals[13].

The algorithm described here greatly facilitates the analysis of local Ca^{2+} signals from camera based imaging. By automating identification and analysis not only is user bias eliminated, but gigabytes of image stacks can be processed within minutes in a highly parallel fashion, yielding both temporal and spatial data from multiple events from a single-cell simultaneously.

Although data in this manuscript are presented in the context of IP_3-mediated Ca^{2+} signals, the approaches described can be readily extended to imaging local changes in cytosolic $[Ca^{2+}]$ emanating from numerous types of ligand-, second-messenger- and voltage-gated Ca^{2+}-permeable ion channels. The high-throughput nature of the algorithm for automating identification and analysis of local Ca^{2+} events should also prove to be highly useful for imaging Ca^{2+} channelopathies in disease states via single-cell models such as Alzheimer's disease and autism spectrum disorder.

Disclosures

The authors declare that they have no competing financial interests.

Acknowledgements

References

1. Berridge, M. J., Lipp, P., Bootman, M. D. The versatility and universality of calcium signalling. *Nat Rev Mol Cell Biol.* **1**, (1), 11-21 (2000).
2. Hill-Eubanks, D. C., Werner, M. E., Heppner, T. J., Nelson, M. T. Calcium signaling in smooth muscle. *Cold Spring Harb Perspect Biol.* **3**, (9), a004549 (2011).
3. Hagenston, A. M., Bading, H. Calcium signaling in synapse-to-nucleus communication. *Cold Spring Harb Perspect Biol.* **3**, (11), a004564 (2011).
4. Berridge, M. J. Elementary and global aspects of calcium signalling. *J Physiol.* **499**, (Pt 2), 291-306 (1997).
5. Lipp, P., Niggli, E. A hierarchical concept of cellular and subcellular calcium signalling). *Prog Biophys Mol Biol.* **65**, (3), 265-296 (1996).
6. Parker, I., Yao, Y., Ilyin, V. Fast kinetics of calcium liberation induced in Xenopus oocytes by photoreleased inositol trisphosphate. *Biophys J.* **70**, (1), 222-237 (1996).
7. Minta, A., Kao, J. P., Tsien, R. Y. Fluorescent indicators for cytosolic calcium based on rhodamine and fluorescein chromophores. *J Biol Chem.* **264**, (14), 8171-8178 (1989).
8. Demuro, A., Parker, I. Imaging the activity and localization of single voltage-gated Ca(2+) channels by total internal reflection fluorescence microscopy. *Biophys J.* **86**, (5), 3250-3259 (2004).
9. Smith, I. F., Parker, I. Imaging the quantal substructure of single inositol trisphosphate receptor channel activity during calcium puffs in intact mammalian cells. *Proc Natl Acad Sci U S A.* **106**, (15), 6404-6409 (2009).
10. Reissner, K. J., *et al.* A novel postsynaptic mechanism for heterosynaptic sharing of short-term plasticity. *J Neurosci.* **30**, (26), 8797-8806 (2010).
11. Ellefson, K. S., Parker, B., Smith, I., F, I. An algorithm for automated detection, localization and measurement of local calcium signals from camera-based imaging. *Cell Calcium.* (2014).
12. Smith, I. F., Wiltgen, S. M., Parker, I. Localization of puff sites adjacent to the plasma membrane: Functional and spatial characterization of calcium signaling in SH-SY5Y cells utilizing membrane-permeant caged inositol trisphosphate. *Cell Calcium.* **45**, 65-76 (2009).
13. Shuai, J., Parker, I. Optical single-channel recording by imaging calcium flux through individual ion channels: theoretical considerations and limits to resolution. *Cell Calcium.* **37**, (4), 283-299 (2005).